Atmos. Chem. Phys. Discuss., 13, 19625–19648, 2013
www.atmos-chem-phys-discuss.net/13/19625/2013/
doi:10.5194/acpd-13-19625-2013

Atmospheric Chemistry and Physics Discussions

Sources and light absorption of water-soluble brown carbon aerosols in the outflow from northern China

E. N. Kirillova[1], A. Andersson[1], J. Han[2], M. Lee[2], and Ö. Gustafsson[1]

[1]Department of Applied Environmental Science (ITM) and the Bolin Centre for Climate Research, Stockholm University, 106 91 Stockholm, Sweden
[2]Department of Earth and Environmental Sciences, Korea University, 136-701 Seoul, South Korea

Received: 9 July 2013 – Accepted: 10 July 2013 – Published: 25 July 2013

Correspondence to: Ö. Gustafsson (orjan.gustafsson@itm.su.se)

Published by Copernicus Publications on behalf of the European Geosciences Union.

Abstract

High loadings of anthropogenic carbonaceous aerosols in Chinese air influence the air quality for over 1 billion people and impact the regional climate. A large fraction (17–80 %) of this aerosol carbon is water soluble, promoting cloud formation and thus climate cooling. Recent findings, however, suggest that water-soluble carbonaceous aerosols also absorb sunlight, bringing additional direct and indirect climate warming effects, yet the extent and nature of light absorption by this water-soluble brown carbon (WS-BrC) and its relation to sources is poorly understood. Here, we combine source estimates constrained by dual-carbon-isotope with light absorption measurements of WS-BrC for a March 2011 campaign at the Korea Climate Observatory at Gosan (KCOG), a receptor station in SE Yellow Sea for the outflow from N. China. The mass absorption cross-section (MAC) of WS-BrC for air masses from N. China were in general higher (0.8–1.1 $m^2\,g^{-1}$), than from other source regions (0.3–0.8 $m^2\,g^{-1}$). We estimate that this effect corresponds to 13–49 % of the radiative forcing caused by light absorption by black carbon. Radiocarbon constraints show that the WS-BrC in Chinese outflow had significantly higher amounts of fossil sources (30–50 %) compared to previous findings in S. Asia, N. America and Europe. Stable carbon ($\delta^{13}C$) measurements indicated influence of aging during air mass transport. These results indicate the importance of incorporating WS-BrC in climate models and the need to constrain climate effects by emission source sector.

1 Introduction

High emissions of anthropogenic carbon aerosols from highly industrialized and populated northern and eastern China (Fig. 1) greatly influence the regional climate and air quality of the whole East Asian region. The water-soluble organic carbon (WSOC) is a substantial component of East Asian aerosols with estimates spanning from 17–80 % of the total organic carbon (TOC) (Feng et al., 2006, 2007; Duvall et al., 2008;

ACPD
13, 19625–19648, 2013

Pathak et al., 2011; Huang et al., 2012). WSOC may influence regional climate through several mechanisms. WSOC affects the particle's hygroscopicity and hence the ability of aerosol particles to act as cloud condensation nuclei (CCN) thus contributing to the indirect aerosol climate effects (e.g., Charlson et al., 2001; Svenningsson et al., 2006; Asa-Awuku et al., 2008). It has recently been found that WSOC exhibits light-absorbing ("brown carbon" BrC) properties (Cheng et al., 2011; Zhang et al., 2011). This WS-BrC contributes both a direct climate forcing (Chung et al., 2012; Bahadur et al., 2012; Jacobson, 2012) and a semi-direct climate effect through heating and evaporation of clouds (Jacobson, 2012).

There is a need to better understand the sources, properties and atmospheric processing of WS-BrC. It has been suggested that WSOC in atmospheric particles may come from a wide range of primary and secondary sources (e.g., Decesari et al., 2007; de Gouw et al., 2008). A few initial studies with direct measurement of the natural abundance radiocarbon content of WSOC appears promising to constrain the sources of this large aerosol carbon fraction. Short-term radiocarbon-based studies of WSOC in N. America and Europe suggest an overwhelming contribution of modern carbon sources to WSOC in both rural and urban environment (Szidat et al., 2004; Weber et al., 2007; Wozniak et al., 2008, 2012a, b; Kirillova et al., 2010). However, recent year-round ^{14}C-WSOC campaigns at two regional background sites constrained a 20 % fossil contribution in S. Asia (Kirillova et al., 2013). Given the larger contribution of fossil-fuel combustion to elemental carbon (EC) in E. Asia than in S. Asia (Zhang et al., 2009; Ramana et al., 2010), it is conceivable that there is a substantially larger contribution by anthropogenic-fossil sources also to WSOC (and thus WS-BrC) over East Asia.

Furthermore, the stable carbon isotope signal (δ^{13}C) can be used to differentiate not only sources but also the atmospheric processing of the carbonaceous aerosols as it additionally reflects kinetic isotope effects (KIE) induced by transformation reactions during both primary aerosol and precursor emissions as well as during atmospheric transport (Anderson et al., 2004; Widory et al., 2006; Aggarwal and Kawamura, 2008; Das et al., 2010; Iannone et al., 2010; Kirillova et al., 2013).

ACPD
13, 19625–19648, 2013

In this paper we present light absorbing properties and carbon isotope-constrained source apportionment of WS-BrC from the Gosan Pollution Experiment (GoPoEx), performed at the Korea Climate Observatory at Gosan (KCOG), Jeju Island, SE Yellow Sea in March 2011. These findings emphasize the stronger light absorption and more fossil sources of WS-BrC in Chinese outflow compared with other regions.

2 Materials and methods

2.1 Sampling site and sampling program

The Gosan Pollution Experiment (GoPoEx) was conducted at the Korea Climate Observatory at Gosan (KCOG, 72 m a.s.l., 33.17° N, 126.10° E) during 8–27 March 2011. KCOG is located in a rural area at the western tip of Jeju Island, 100 km south of the Korean peninsula (Fig. 1), and is a part of ACE-Asia (Huebert et al., 2003), Advanced Global Atmospheric Gases Experiment (AGAGE, http://agage.eas.gatech.edu/), Global Atmosphere Watch (GAW) program (http://www.wmo.int/pages/prog/arep/gaw/gaw_home_en.html), and the International Atmospheric Brown Cloud (ABC) project (http://www.rrcap.unep.org/abc/). During GoPoEx, measurements of gaseous components (e.g., CO and SO_2) and bulk particulate parameters (e.g., $PM_{2.5}$, PM_{10}, elemental carbon (EC)) as well as meteorology descriptors were collected at high frequency (averaged to ≤ 1 h, Fig. 2). These measurements, in conjunction with HYSPLIT forecast BTs and weather maps from the Korean Meteorological Association (KMA) were used to guide the high-volume filter sampling, with the aim of obtaining source-region specific filter collections. Aerosols were collected on pre-combusted quartz-fiber filters using high volume $PM_{2.5}$ (model DH77, Digitel A.G., Switzerland) and TSP samplers. The filter samples (1–26) collected during the campaign (Fig. 2, Supplement Table S1) were analyzed for concentrations, isotope compositions and optical properties of the carbonaceous aerosols.

ACPD
13, 19625–19648, 2013

2.2 Analysis of carbonaceous aerosol fractions

The aerosol total organic carbon (TOC) concentrations were measured with a thermal-optical transmission (TOT) analyzer (Sunset Laboratory, Tigard, OR, USA) using the standard NIOSH 5040 method (Birch and Cary, 1996). TOC concentration values were blank corrected and the field blank input was on average 10 % (1.19 ± 0.34 s.d., $\mu g\,cm^{-2}$; $n = 4$) for TSP and 11 % (0.74 ± 0.08 s.d., $\mu g\,cm^{-2}$; $n = 4$) for $PM_{2.5}$. The average relative standard deviation of triplicate analysis was 7 % for TSP and 11 % for $PM_{2.5}$. WSOC was extracted by ultrasonication and quantified by a high-temperature catalytic instrument (Shimadzu-TOC-VCPH, Japan) as described previously (Kirillova et al., 2010). All WSOC results were blank corrected by subtracting an average field blank value. The WSOC field blanks corresponded to an average 6 % (0.30 ± 0.06 s.d., $\mu g\,cm^{-2}$; $n = 3$) for TSP and 7 % (0.20 ± 0.01 s.d., $\mu g\,cm^{-2}$; $n = 3$) for $PM_{2.5}$ of the field sample loading. Triplicate analysis was done on three TSP and four $PM_{2.5}$ filters. The average relative standard deviation of triplicate analysis was 4 % for TSP and 6 % for $PM_{2.5}$.

2.3 Carbon isotope analysis

Ten samples were chosen for carbon isotope analysis based on an air mass origin from China and sufficient carbon loadings as described in Supplement.

2.3.1 TOC

The carbon aerosol TOT analyzer was slightly modified for online isolation of CO_2 produced during the combustion of a sample for further measurements of ^{13}C and ^{14}C. First, a filter area corresponding to at least 100 µg TOC for each sample was acidified by fumigation in open glass Petri dishes held in a desiccator over 12 M hydrochloric acid for 24 h to remove carbonates and subsequently dried at 60 °C for 1 h. The total carbon method was used on the TOT instrument to isolate the entire TOC for subsequent

ACPD
13, 19625–19648, 2013

radiocarbon analysis. During this method a 1.5 cm^2 subsample was heated at the two ramps to 870 °C in the atmosphere of helium (98 %) and oxygen (2 %) during 110 s and remained to be exposed to the temperature of 870 °C for 190 s until all the TOC was oxidized to CO_2.

The CO_2 produced by the TOT analyzer was purified through magnesium perchlorate and silver wool traps to remove water and halogen-containing gases, correspondingly. Subsequently, it was cryotrapped in liquid N_2 and sealed in the glass ampoules. Further, the CO_2 was reduced to graphite, and the carbon isotopic composition was measured at the US NSF National Ocean Science Accelerator Mass Spectrometry (NOSAMS) facility (Woods Hole, MA, USA).

2.3.2 WSOC

For ^{13}C and ^{14}C analysis a filter area corresponding to at least 150 µg WSOC for each of 10 chosen samples was acidified by fumigation as described above and extracted as described previously (Kirillova et al., 2010). Stable carbon isotope ($\delta^{13}C$-WSOC) measurements were performed at the Stable Isotope Laboratory (SIL) of the Department of Geological Sciences at Stockholm University (Stockholm, Sweden). The instrumental method employed sample combustion with a Carlo Erba NC2500 analyzer connected via a split interface to reduce the gas volume to a Finnigan MAT Delta V mass spectrometer. The radiocarbon measurements of the freeze-dried WSOC isolates were performed at the US-NSF NOSAMS facility as described previously (McNichol et al., 1992; Pearson et al., 1998; Kirillova et al., 2010).

2.4 Uncertainty estimation

The overall precision of TC and WSOC concentrations and isotopic signatures was estimated based on uncertainties from several different sources, including the precision of concentration estimation (estimates from triplicate analysis), mass contributions from field blanks (estimates from several blanks), as well as precision of isotope

ACPD
13, 19625–19648, 2013

characterization (instrument precision) and the isotope signature of the field blanks (Supplement). To properly account for all uncertainties, we employed an error propagation scheme based on a Monte Carlo strategy as described previously (Kirillova et al., 2013).

2.5 Light absorption by WS-BrC

Light extinction of 13 WSOC samples (both TSP and $PM_{2.5}$) was measured using a Hitachi U2010 spectrophotometer, using the wavelength range of 190–1100 nm. The mass absorption cross section (MAC) was computed according to the Lambert–Beer Law:

$$\mathrm{MAC} = \frac{-\ln\left|\frac{I}{I_0}\right|}{C \cdot L} = \frac{A}{C \cdot L} \quad (1)$$

Where I denote light intensity, C is the concentration of WSOC in solution, L is the light path length (= 1 cm, for the currently used quartz cuvettes) and A is the absorbance (assuming that the scattering contribution to extinction is low). For comparison with previous results, the MAC was computed for 365 nm (Cheng et al., 2011). Equation (1) predicts a linear relation between absorbance and concentration. This prediction was tested by dilution experiments, and was found to agree well within the currently investigated concentration/wavelength range (data not shown).

The wavelength (λ) dependence of the WSOC absorption was investigated by fitting an absorption Ångström Exponent (AAE) using the following relation:

$$\frac{A(\lambda_1)}{A(\lambda_2)} = \left(\frac{\lambda_1}{\lambda_2}\right)^{\mathrm{AAE}} \quad (2)$$

AAE were fitted within the range 330–400 nm to avoid interference from light absorbing inorganic compounds such as nitrate (Cheng et al., 2011).

ACPD
13, 19625–19648, 2013

3 Results and discussion

3.1 Meteorological setting and air mass characterization

The climate of Jeju Island is driven by the Asian monsoon system. In late winter and spring, the air masses arriving at KCOG are largely influenced by the anthropogenic activities in China and Korea, and by Asian dust storms (e.g., Carmichael et al., 1996; Huebert et al., 2003; Sahu et al., 2009). The major objective of the Gosan Pollution Experiment (GoPoEx), carried out at KCOG 8–23 March 2011, was to intercept aerosols from the N. Chinese outflow to study their sources and properties.

To examine the geographical source regions of the air masses during GoPoEx, five-day back trajectories (BTs) were generated at three arrival heights (100, 500 and 850 m a.g.l.) for every 6 h using NOAA HYSPLIT software v4 (http://www.arl.noaa.gov/ready/hysplit4.html). Consideration of both path and heights of the BTs allowed us to determine five main source areas: Beijing, Liaoning, Yellow Sea, Mongol (Mongolia and the Nei Mongol province of China) and the Korean peninsula (Fig. 1, Supplement, Figs. S1–S3). The air in the Yellow Sea category circulated for extended times at high altitude over Jeju region before descending to KCOG, whereas air mass transfer over the other source regions occurred at low altitudes.

Three episodes of elevated pollutant loadings were observed during the high-intensity campaign (Fig. 2): (1) a pollution event was observed from 10 p.m. of 10 March to 6 a.m. of 12 March (filter samples 5–7) with air-masses originating from the Beijing area, which was characterized by high loadings of $PM_{2.5}$, PM_{10}, EC and SO_2. (2) An Asian dust episode was observed from 5 a.m. of 15 March to 9 a.m. of 16 March (filter samples 13–15), originating from the Mongol source sector, which was characterized by high PM_{10}, low $PM_{2.5}$ and pollution tracers and high wind speeds (13–16 m s^{-1}). (3) A second dust event combined with rain was observed from 1 p.m. of 21 March to the end of campaign (filter samples 25 and 26).

ACPD
13, 19625–19648, 2013

3.2 WSOC abundance and distribution

During GoPoEx, WS-BrC contributed ~ 45–47 % of TOC (Fig. 2c). When comparing total suspended particles (TSP) with $PM_{2.5}$, ~ 80 % of WSOC was found in the fine (< 2.5 µm) mode. The highest concentrations were found during the pollution event (10–12 March, 2.3 µg m^{-3} in $PM_{2.5}$ and 3.5 µg m^{-3} in TSP, Fig. 2), but elevated WSOC concentrations were also observed during the two dust events (15–16 and 21–22 March). The concentrations of WSOC during the GoPoEx period are within the range of what has been observed in Chinese cities (0.4–9.6 µg m^{-3} for $PM_{2.5}$), the concentrations at KCOG during the pollution event are typical of levels reported for Chinese cities (Feng et al., 2006; Pathak et al., 2011; Huang et al., 2012; Cheng et al., 2011).

3.3 Light absorption of water-soluble brown carbon (WS-BrC) in outflow from N. China

Black carbon (BC) is frequently referred to as the major light absorbing aerosol species (e.g., Ramanathan and Carmichael, 2008; Bond et al., 2013). However, other carbonaceous aerosols may also absorb light, but typically with a more pronounced wavelength dependence – "brown carbon" (Andreae and Gelencsér, 2006). For the GoPoEx, the light absorption of WS-BrC was found to have a wavelength dependence reflected in an Absorption Ångström Exponent (AAE) ranging between 5.6 and 7.7 (6.4 ± 0.6, Supplement Fig. S4). In comparison, the AAE for BC is typically 1 (Hecobian et al., 2010; Cheng et al., 2011; Kirchstetter and Thatcher, 2012). The WS-BrC AAE for GoPoEx is comparable with observations near Beijing, China of 7.0 in summer and 7.5 in winter (Cheng et al., 2011), values of 6.2–8.3 in SE USA (Hecobian et al., 2010), 7.1 over the Amazonas (Hoffer et al., 2006). Similarly, the current range of the recipient-intercepted WS-BrC mass absorption cross section values at 365 nm (MAC_{365}) (Fig. 3a) were 0.3–1.1 m^2 g^{-1} (0.7 ± 0.2 m^2 g^{-1}), which compares with Beijing source area during winter (1.8 ± 0.2; Cheng et al., 2011), Beijing in summer (0.7 m^2 g^{-1}; Cheng et al., 2011) and with SE USA (0.3–0.7 m^2 g^{-1}; Hecobian et al., 2010).

ACPD
13, 19625–19648, 2013

Higher MAC_{365} values were observed for samples of Chinese origins (Beijing and Liaoning), including the Beijing area pollution plume, than for Mongol and Korea source regions and dust events (Fig. 3a). Samples attributed to the Yellow Sea group are characterized by lower absorbance (MAC) although initially they were influenced by the emissions from Beijing and Liaoning. The relatively lower MAC_{365} for these samples may reflect bleaching of WS-BrC during circulation above the Yellow Sea. A bleaching effect of WS-BrC during long-range transport is also suggested in the comparison of the MAC from Beijing-winter compared with KCOG recipient values. Taken together, this indicates that WS-BrC originating from anthropogenic emissions from China absorbs more light per mass carbon, than, e.g., WS-BrC from natural sources and may become less absorptive during long-range transport.

To estimate the relative range of climate warming potential due to light absorption of WS-BrC compared to BC a simplistic calculation of absorption-based radiative forcing was employed (Supplement for details). The relative absorption-based radiative forcing was calculated as the wavelength-dependent integrated product of solar emission and WS-BrC light absorption attenuation divided by the analogous integral for BC (Supplement Fig. S6). The amount of solar energy absorbed by WS-BrC relative to BC was 13–49 % during the GoPoEx (Fig. 3b), with higher values for the fine aerosols ($PM_{2.5}$). This estimation shows that WS-BrC has the potential to contribute to significant warming, which may partly counteract the scattering caused by aerosols and clouds. Additionally and not included in this simple calculation, WS-BrC in cloud droplets may also induce cloud burn off (e.g., Jacobson, 2012). Since the multiple climate effects of WS-BrC may be modulated by bleaching during long-range transport, careful modeling is required to better resolve the direct and indirect climate effects of these species.

3.4 Sources and atmospheric processing of WS-BrC

Radiocarbon ($\Delta^{14}C$) has recently been shown to be a powerful technique for differentiating biomass vs fossil sources for different components of Asian carbonaceous aerosols (e.g., Gustafsson et al., 2009; Sheesley et al., 2012; Kirillova et al., 2013). For

ACPD
13, 19625–19648, 2013

GoPoEx, radiocarbon measurements of WS-BrC show that the fossil contribution is as large as the biomass contribution in the $PM_{2.5}$ fraction (Fig. 3c). These values are much higher than what has previously been reported for WSOC in Europe and USA, showing the much larger influence of fossil sources to this large component of aerosol carbon in the N. China outflow. For TSP, the fossil contribution was somewhat lower, showing a large influence from biomass/biogenic coarse mode water soluble particles. Little variation in time was found during the present campaign, except for the dust episodes, when then biomass contribution was larger.

By combining the $\Delta^{14}C$ with the stable carbon isotope ($\delta^{13}C$) composition, it is possible to examine the dual effects of source variability and atmospheric processing of WS-BrC as well as of TOC (Kirillova et al., 2013). Since the $\Delta^{14}C$ parameter is reported relative to a stable carbon standard, this parameter is only sensitive to emission source (biomass vs fossil) variability. In contrast, $\delta^{13}C$ is sensitive to both variability of different emissions sources (e.g., coal, petroleum, wood combustion and marine sources) and to atmospheric processing due to the kinetic isotope effect. By considering the two-dimensional $\Delta^{14}C$-$\delta^{13}C$ signal for the GoPoEx campaign, four distinct clusters appear in the following order (from lower left to top right along the E. Asia continuum in Fig. 4): TOC $PM_{2.5}$, TOC TSP, WS-BrC $PM_{2.5}$ and WS-BrC TSP. The four populations are distributed along a straight line, which is very similar to our previous findings for the S. Asian outflow (Fig. 4: S. Asia continuum line, Kirillova et al., 2013). Comparison of the E. Asian and S. Asian datasets show three consistent trends: (1) Higher fossil contribution in both WS-BrC and TOC in E. Asia than in S. Asia; (2) WS-BrC is more modern (i.e., "younger" ^{14}C signal) and more enriched in ^{13}C compared to TOC in both size fractions for both E. and S. Asia; (3) Coarse particles are more modern and enriched in ^{13}C compared to $PM_{2.5}$ for both WS-BrC and TOC.

The enrichment in ^{13}C of WS-BrC relative to TOC in both E. and S. Asia may reflect either difference in sources or in atmospheric processing. Particulate emission sources cover a wide range of $\delta^{13}C$ values: on average −13 ‰ for C4 plants, −22 to −18 ‰ for marine sources, −23 to −21 ‰ for coal, −34 to −25 ‰ for C3 plants, −29 to −24 ‰

ACPD
13, 19625–19648, 2013

for liquid petroleum and −40 to −28 ‰ for gaseous petroleum (e.g., Miyazaki et al., 2007, 2011; Kawashima and Haneishi, 2012; Anghitori et al., 2011; Widory, 2006). For Chinese outflow, C4 plants (e.g., maize and sugar cane) are not expected to be a large contribution. By combining the isotope data with ratios of inorganic ions isolated from the same filters, marine sources are not expected to have a major influence on WS-BrC during the GoPoEx (Fig. S7).

The $\delta^{13}C$ value is also influenced by atmospheric processing (Fig. 4 inset). During formation of Secondary Organic Aerosol (SOA), molecules depleted in heavy isotopes are expected to react faster, leading to depletion in ^{13}C. This prediction is supported by laboratory studies (e.g., Iannone et al., 2010; Anderson et al., 2004). In contrast, during atmospheric aging (here meaning reactions with reactive species such as the hydroxyl radical) molecules with lighter isotopes react faster, forming gaseous species such as CO, CO_2 and volatile organic carbon (VOCs). This leads to an enrichment of ^{13}C in the residual carbon in the aerosol phase, which has also been supported by laboratory and field studies (Aggarwal and Kawamura, 2008; Smith et al., 2009). In addition, aging may also involve rearrangement within the aerosol phase, e.g. condensation reactions, without production of gaseous substances (Kalberer et al., 2004; Zahardis et al., 2006; Nguyen et al., 2011). Since there is then no net transfer of carbon, these reactions do not affect $\delta^{13}C$ signature of the aerosol TOC, but may change the signature of a sub-population such as of the WS-BrC. Semivolatile organic compounds partition between gas and particulate phases causing enrichment of heavier isotopes in the particulate phase. However, laboratory studies indicate these effects are likely to have only a minor effect on the $\delta^{13}C$ signature (Harrington et al., 1999; Wang and Kawamura, 2006).

Both SOA formation and aging leads to production of more polar compounds, such as WS-BrC. The higher $\delta^{13}C$ values (^{13}C enrichment) of WS-BrC compared with TOC either indicates differences in sources or processing. Excluding the less likely candidates C4 plants and marine contributions, it is unlikely that the observed difference between TOC and WS-BrC reflects source differences. Instead, the more probable explanation is that this difference is explained by atmospheric processing/aging since

ACPD
13, 19625–19648, 2013

enrichment in ^{13}C is observed (Kirillova et al., 2013). This hypothesis is consistent with the fact that the same TOC vs WS-BrC trend is observed at all three sites (KCOG, MCOH and SINH) and for two size fractions ($PM_{2.5}$ and TSP) (Fig. 4), as well as WS-BrC being more polar than TOC in general. The more enriched ^{13}C values observed at MCOH (S. Asia receptor), compared with SINH and KCOG, are likely to reflect a longer source-receptor transport time.

The enrichment in ^{13}C observed in WS-BrC relative to TOC is for the currently examined datasets always correlated with higher biomass ($\Delta^{14}C$ value) contents. Fossil combustion in general occurs at higher temperatures/pressures than biomass burning. This means that fossil sources of carbonaceous aerosols are more recalcitrant to further chemical oxidation than products of biomass burning and biogenic origins (Elmquist et al., 2006). This observation thus offers an explanation why "aging" (here in the meaning of reactive transformations) of carbonaceous aerosols is preferential for more ^{14}C-modern (i.e., biomass) components. In addition, atmospheric processing also offers an explanation why $PM_{2.5}$ particles are more depleted in ^{13}C than TSP: SOA formation produces particles that rarely grow larger than 2.5 µm (Seinfeld and Pandis, 1998). The lower $\delta^{13}C$ of $PM_{2.5}$ for both TOC and WS-BrC are thus expected to reflect larger relative contributions from SOA to the WS-BrC in $PM_{2.5}$ than in the TSP pool.

4 Conclusions

Radiocarbon (^{14}C) constraints of carbonaceous aerosols in Chinese outflow show that about 50 % of water soluble Brown Carbon (WS-BrC) is of fossil origins. This contribution is significantly larger than what has been observed in S. Asia, Europe and USA. The direct light absorptive properties of WS-BrC were found to range 13–49 % relative to that of the main light absorptive aerosol species, black carbon, with even higher values for the fine aerosol fraction. Stable carbon isotope analysis show that the WS-BrC from the Chinese outflow observed at the Yellow Sea receptor site is subject to aging during long-range transport, which may be related to the bleaching inferred

ACPD
13, 19625–19648, 2013

from a lower mass absorption coefficient at the receptor site compared to reports from Chinese cities. These results suggests the need, yet challenge, to incorporate the heterogeneous WS-BrC in climate models as well as the need to constrain climate effects of non-BC light-absorbing species by both emission source sector and possibly by extent of aging.

Supplementary material related to this article is available online at: http://www.atmos-chem-phys-discuss.net/13/19625/2013/acpd-13-19625-2013-supplement.pdf.

Acknowledgements. We are grateful to the PI team of the Korea Climate Observatory at Gosan (KCOG) for maintaining a well-equipped station and for graciously granting access during the GoPoEx. The authors acknowledge financial support from the Swedish Research Council for Environment, Agricultural Sciences and Spatial Planning (FORMAS Contract no. 214-2009-970) STINT Foundation (Nr. 2010/072) and the Korean Center for Atmospheric and Earthquake Research. ÖG also acknowledges financial support as an Academy Researcher from the Swedish Royal Academy of Sciences through a grant from the Knut and Alice Wallenberg Foundation. AA acknowledges financial support from the Knut and Alice Wallenberg Foundation. This study also benefitted from the research environments provided by the Bolin Centre for Climate Research and the Delta Facility (a core facility for compound-specific isotope analysis), both at the Stockholm University, School of Natural Sciences.

References

Aggarwal, S. G. and Kawamura, K.: Molecular distributions and stable carbon isotopic compositions of dicarboxylic acids and related compounds in aerosols from Sapporo, Japan: implications for photochemical aging during long-range atmospheric transport, J. Geophys. Res., 113, D14301, doi:10.1029/2007JD009365, 2008.

ACPD
13, 19625–19648, 2013

Agnihotri, R., Mandal, T. K., Karapurkar, S. G., Naja, M., Gadi, R., Ahammmed, Y. N., Kumar, A., Saud, T., and Saxena, M.: Stable carbon and nitrogen isotopic composition of bulk aerosols over India and northern Indian Ocean, Atmos. Environ., 45, 2828–2835, 2011.

Anderson, R. S., Iannone, R., Thompson, A. E., Rudolph, J., and Huang, L.: Carbon kinetic isotope effects in the gas-phase reactions of aromatic hydrocarbons with the OH radical at 296 ± 4 K, Geophys. Res. Lett., 31, L15108, doi:10.1029/2004GL020089, 2004.

Andreae, M. O. and Gelencsér, A.: Black carbon or brown carbon? The nature of light-absorbing carbonaceous aerosols, Atmos. Chem. Phys., 6, 3131–3148, doi:10.5194/acp-6-3131-2006, 2006.

Asa-Awuku, A., Sullivan, A. P., Hennigan, C. J., Weber, R. J., and Nenes, A.: Investigation of molar volume and surfactant characteristics of water-soluble organic compounds in biomass burning aerosol, Atmos. Chem. Phys., 8, 799–812, doi:10.5194/acp-8-799-2008, 2008.

Bahadur, R., Praveen, P. S., Xu, Y., and Ramanathan, V.: Solar absorption by elemental and brown carbon determined from spectral observations, P. Natl. Acad. Sci. USA, 109, 17366–17371, 2012.

Birch, M. E. and Cary, R. A.: Elemental carbon-based method for monitoring occupational exposures to particulate diesel exhaust, Aerosol Sci. Tech., 25, 221–241, 1996.

Bond, T. C., Doherty, S. J., Fahey, D. W., Forster, P. M., Berntsen, T., DeAngelo, B. J., Flanner, M. G., Ghan, S., Kärcher, B., Koch, D., Kinne, S., Kondo, Y., Quinn, P. K., Sarofim, M. C., Schultz, M. G., Schulz, M., Venkataraman, C., Zhang, H., Zhang, S., Bellouin, N., Guttikunda, S. K., Hopke, P. K., Jacobson, M. Z., Kaiser, J. W., Klimont, Z., Lohmann, U., Schwarz, J. P., Shindell, D., Storelvmo, T., Warren, S. G., and Zender, C. S.: Bounding the role of black carbon in the climate system: A scientific assessment, J. Geophys. Res.-Atmos., 118, 5380–5552, doi:10.1002/jgrd.50171, 2013.

Carmichael, G. R., Zhang, Y., Chen, L.-L., Hong, M.-S., and Uedas, H.: Seasonal variation of aerosol composition at Cheju Island, Korea, Atmos. Environ., 30, 2407–2416, 1996.

Charlson, R. J., Seinfeld, J. H., Nenes, A., Kulmala, M., Laaksonen, A., and Facchini, M. C.: Atmospheric science – reshaping the theory of cloud formation, Science, 292, 2025–2026, 2001.

Cheng, Y., He, K.-B., Zheng, M., Duan, F.-K., Du, Z.-Y., Ma, Y.-L., Tan, J.-H., Yang, F.-M., Liu, J.-M., Zhang, X.-L., Weber, R. J., Bergin, M. H., and Russell, A. G.: Mass absorption efficiency of elemental carbon and water-soluble organic carbon in Beijing, China, Atmos. Chem. Phys., 11, 11497–11510, doi:10.5194/acp-11-11497-2011, 2011.

ACPD
13, 19625–19648, 2013

Chung, C. E., Ramanathan, V., and Decremer, D.: Observationally constrained estimates of carbonaceous aerosol radiative forcing, P. Natl. Acad. Sci. USA, 109, 11624–11629, 2012.
Das, O., Wang, Y., and Hsieh, Y.-P.: Chemical and carbon isotopic characteristics of ash and smoke derived from burning of C-3 and C-4 grasses, Org. Geochem., 41, 263–269, 2010.
de Gouw, J. A., Brock, C. A., Atlas, E. L., Bates, T. S., Fehsenfeld, F. C., Goldan, P. D., Holloway, J. S., Kuster, W. C., Lerner, B. M., Matthew, B. M., Middlebrook, A. M., Onasch, T. B., Peltier, R. E., Quinn, P. K., Senff, C. J., Stohl, A., Sullivan, A. P., Trainer, M., Warneke, C., Weber, R. J., and Williams, E. J.: Sources of particulate matter in the northeastern United States in summer: 1. Direct emissions and secondary formation of organic matter in urban plumes, J. Geophys. Res., 113, D08301, doi:10.1029/2007JD009243, 2008.
Decesari, S., Mircea, M., Cavalli, F., Fuzzi, S., Moretti, F., Tagliavini, E., and Facchini, M. C.: Source attribution of water-soluble organic aerosol by nuclear magnetic resonance spectroscopy, Environ. Sci. Technol., 41, 2479–2484, 2007.
Duvall, R. M., Majestic, B. J., Shafer, M. M., Chuang, P. Y., Simoneit, B. R. T., and Schauer, J. J.: The water-soluble fraction of carbon, sulfur, and crustal elements in Asian aerosols and Asian soils, Atmos. Environ., 42, 5872–5884, 2008.
Elmquist, M., Cornelissen, G., Kukulska, Z., and Gustafsson, Ö.: Distinct oxidative stabilities of char versus soot black carbon: implications for quantification and environmental recalcitrance, Global Biogeochem. Cy., 20, GB2009, doi:10.1029/2005GB002629, 2006.
Feng, J., Hu, M., Chan, C. K., Lau, P. S., Fang, M., He, L., and Tang, X.: A comparative study of the organic matter in $PM_{2.5}$ from three Chinese megacities in three different climatic zones, Atmos. Environ., 40, 3983–3994, 2006.
Feng, J., Guo, Z., Chan, C. K., and Fang, M.: Properties of organicmatter in $PM_{2.5}$ at Changdao Island, China – a rural site in the transport path of the Asian continental outflow, Atmos. Environ., 41, 1924–1935, 2007.
George, I. J. and Abbatt, J. P. D.: Heterogeneous oxidation of atmospheric aerosol particles by gas-phase radicals, Nat. Chem., 2, 713–722, 2010.
Gustafsson, O., Krusa, M., Zencak, Z., Sheesley, R. J., Granat, L., Engstrom, E., Praveen, P. S., Rao, P. S. P., Leck, C., and Rodhe, H.: Brown clouds over South Asia: biomass or fossil fuel combustion?, Science, 323, 495–498, 2009.
Harrington, R. R., Poulson, S. R., Drever, J. I., Colberg, P. J.S, and Kelly, E. F.: Carbon isotope systematics of monoaromatic hydrocarbons: vaporization and adsorption experiments, Org. Geochem., 30, 765–775, 1999.

ACPD
13, 19625–19648, 2013

Hecobian, A., Zhang, X., Zheng, M., Frank, N., Edgerton, E. S., and Weber, R. J.: Water-Soluble Organic Aerosol material and the light-absorption characteristics of aqueous extracts measured over the Southeastern United States, Atmos. Chem. Phys., 10, 5965–5977, doi:10.5194/acp-10-5965-2010, 2010.

Hoffer, A., Gelencsér, A., Guyon, P., Kiss, G., Schmid, O., Frank, G. P., Artaxo, P., and Andreae, M. O.: Optical properties of humic-like substances (HULIS) in biomass-burning aerosols, Atmos. Chem. Phys., 6, 3563–3570, doi:10.5194/acp-6-3563-2006, 2006.

Huang, H., Ho, K. F., Lee, S. C., Tsang, P. K., Ho, S. S. H., Zou, C. W., Zou, S. C., Cao, J. J., and Xu, H. M.: Characteristics of carbonaceous aerosol in $PM_{2.5}$: Pearl Delta River Region, China, Atmos. Res., 104–105, 227–236, 2012.

Huebert, B. J., Bates, T., Russell, P. B., Shi, G., Kim, Y. J., Kawamura, K., Carmichael, G., and Nakajima, T.: An overview of ACE-Asia: strategies for quantifying the relationships between Asian aerosols and their climatic impacts, J. Geophys. Res., 108, D238633, doi:10.1029/2003JD003550, 2003.

Iannone, R., Koppmann, R., and Rudolph, J.: Stable carbon kinetic isotope effects for the production of methacrolein and methyl vinyl ketone from the gas-phase reactions of isoprene with ozone and hydroxyl radicals, Atmos. Environ., 44, 4135–4141, 2010.

Jacobson, M. Z.: Investigating cloud absorption effects: Global absorption properties of black carbon, tar balls, and soil dust in clouds and aerosols, J. Geophys. Res., 117, D06205, doi:10.1029/2011JD017218, 2012.

Kalberer, M., Paulsen, D., Sax, M., Steinbacher, M., Dommen, J., Prevot, A. S. H., Fisseha, R., Weingartner, E., Frankevich, V., Zenobi, R., and Baltensperger, U.: Identification of polymers as major components of atmospheric organic aerosols, Science, 303, 1659–1662, 2004.

Kawashima, H. and Haneishi, Y.: Effects of combustion emissions from the Eurasian continent in winter on seasonal delta C-13 of elemental carbon in aerosols in Japan, Atmos. Environ., 46, 568–579, 2012.

Kirchstetter, T. W. and Thatcher, T. L.: Contribution of organic carbon to wood smoke particulate matter absorption of solar radiation, Atmos. Chem. Phys., 12, 6067–6072, doi:10.5194/acp-12-6067-2012, 2012.

Kirillova, E. N., Sheesley, R. J., Andersson, A., and Gustafsson, Ö.: Natural abundance ^{13}C and ^{14}C analysis of water soluble organic carbon (WSOC) in atmospheric aerosols, Anal. Chem., 82, 7973–7978, 2010.

ACPD
13, 19625–19648, 2013

Kirillova, E. N., Andersson, A., Sheesley, R. J., Krusa, M., Praveen, P. S., Budhavant, K., Safai, P. D., Rao, P. S. P., and Gustafsson, Ö.: ^{13}C- and ^{14}C-based study of sources and atmospheric processing of water-soluble organic carbon (WSOC) in South Asian aerosols, J. Geophys. Res.-Atmos., 118, 614–626, doi:10.1002/jgrd.50130, 2013.

McNichol, A. P., Gagnon, A. R., Jones, G. A., and Osborne, E. A.: Illumination of a black box: analysis of gas composition during graphite target preparation, Radiocarbon, 34, 321–329, 1992.

Miyazaki, Y., Kondo, Y., Han, S., Koike, M., Kodama, D., Komazaki, Y., Tanimoto, H., and Matsueda, H.: Chemical characteristics of water-soluble organic carbon in the Asian outflow, J. Geophys. Res., 112, D22S30, doi:10.1029/2007JD009116, 2007.

Miyazaki, Y., Kawamura, K., Jung, J., Furutani, H., and Uematsu, M.: Latitudinal distributions of organic nitrogen and organic carbon in marine aerosols over the western North Pacific, Atmos. Chem. Phys., 11, 3037–3049, doi:10.5194/acp-11-3037-2011, 2011.

Nguyen, T. B., Roach, P. J., Laskin, J., Laskin, A., and Nizkorodov, S. A.: Effect of humidity on the composition of isoprene photooxidation secondary organic aerosol, Atmos. Chem. Phys., 11, 6931–6944, doi:10.5194/acp-11-6931-2011, 2011.

Pathak, R. K., Wang, T., Ho, K. F., and Lee, S. C.: Characteristics of summertime $PM_{2.5}$organic and elemental carbon in four major Chinese cities: implications of high acidity for water-soluble organic carbon (WSOC), Atmos. Environ., 45, 318–325, 2011.

Pearson, A., McNichol, A. P., Schneider, R. J., Von Reden, K. F., and Zheng, Y.: Microscale AMS (super 14) C measurement at NOSAMS, Radiocarbon, 40, 61–75, 1998.

Ramana, M. V., Ramanathan, V., Feng, Y., Yoon, S.-C., Kim, S.-W., Carmichael, G. R., and Schauer, J. J.: Warming influenced by the ratio of black carbon to sulphate and the black-carbon source, Nat. Geosci., 3, 542–545, 2010.

Ramanathan, V. and Carmichael, G.: Global and regional climate changes due to black carbon, Nat. Geosci., 1, 221–227, 2008.

Sahu, L. K., Kondo, Y., Miyazaki, Y., Kuwata, M., Koike, M., Takegawa, N., Tanimoto, H., Matsueda, H., Yoon, S. C., Kim, Y. J.: Anthropogenic aerosols observed in Asian continental outflow at Jeju Island, Korea, in spring 2005, J. Geophys. Res., 114, D03301, doi:10.1029/2008JD010306, 2009.

Seinfeld, J. H. and Pandis, S. N.: Atmospheric Chemistry and Physics, Wiley, Hoboken, NJ, 1326 pp., 1998.

ACPD
13, 19625–19648, 2013

Sheesley, R. J., Kirillova, E., Andersson, A., Kruså, M., Praveen, P. S., Budhavant, K., Safai, P. D., Rao, P. S. P., and Gustafsson, Ö.: Year-round radiocarbon-based source apportionment 1 of carbonaceous aerosols at two background sites in South Asia, J. Geophys. Res., 117, D10202, doi:10.1029/2011JD017161, 2012.

Smith, J. D., Kroll, J. H., Cappa, C. D., Che, D. L., Liu, C. L., Ahmed, M., Leone, S. R., Worsnop, D. R., and Wilson, K. R.: The heterogeneous reaction of hydroxyl radicals with sub-micron squalane particles: a model system for understanding the oxidative aging of ambient aerosols, Atmos. Chem. Phys., 9, 3209–3222, doi:10.5194/acp-9-3209-2009, 2009.

Svenningsson, B., Rissler, J., Swietlicki, E., Mircea, M., Bilde, M., Facchini, M. C., Decesari, S., Fuzzi, S., Zhou, J., Mønster, J., and Rosenørn, T.: Hygroscopic growth and critical supersaturations for mixed aerosol particles of inorganic and organic compounds of atmospheric relevance, Atmos. Chem. Phys., 6, 1937–1952, doi:10.5194/acp-6-1937-2006, 2006.

Szidat, S., Jenk, T. M., Gaggeler, H. W., Synal, H. A., Fisseha, R., Baltensperger, U., Kalberer, M., Samburova, V., Wacker, L., Saurer, M., Schwikowski, M., and Hajdas, I.: Source apportionment of aerosols by C-14 measurements in different carbonaceous particle fractions, Radiocarbon, 46, 475–484, 2004.

Wang, H. and Kawamura, K.: Stable carbon isotopic composition of low-molecular-weight dicarboxylic acids and ketoacids in remote marine aerosols, J. Geophys. Res., 111, D07304, doi:10.1029/2005JD006466, 2006.

Weber, R. J., Sullivan, A. P., Peltier, R. E., Russell, A., Yan, B., Zheng, M., de Gouw, J., Warneke, C., Brock, C., Holloway, J. S., Atlas, E. L., and Edgerton, E.: A study of secondary organic aerosol formation in the anthropogenic-influenced southeastern United States, J. Geophys. Res., 112, D13302, doi:10.1029/2007JD008408, 2007.

Widory, D.: Combustibles, fuels and their combustion products: a view through carbon isotopes, Combust. Theor. Model., 10, 831–841, 2006.

Wozniak, A. S., Bauer, J. E., Sleighter, R. L., Dickhut, R. M., and Hatcher, P. G.: Technical Note: Molecular characterization of aerosol-derived water soluble organic carbon using ultrahigh resolution electrospray ionization Fourier transform ion cyclotron resonance mass spectrometry, Atmos. Chem. Phys., 8, 5099–5111, doi:10.5194/acp-8-5099-2008, 2008.

Wozniak, A. S., Bauer, J. E., and Dickhut, R. M.: Characteristics of water-soluble organic carbon associated with aerosol particles in the eastern United States, Atmos. Environ., 46, 181–188, 2012a.

ACPD
13, 19625–19648, 2013

Wozniak, A. S., Bauer, J. E., Dickhut, R. M., Xu, L., and McNichol, A. P.: Isotopic characterization of aerosol organic carbon components over the eastern United States, J. Geophys. Res., 117, D13303, doi:10.1029/2011JD017153, 2012b.

Zahardis, J., LaFranchi, B. W., and Petrucci, G. A.: Direct observation of polymerization in the oleic acid–ozone heterogeneous reaction system by photoelectron resonance capture ionization aerosol mass spectrometry, Atmos. Environ., 40, 1661–1670, 2006.

Zhang, Q., Streets, D. G., Carmichael, G. R., He, K. B., Huo, H., Kannari, A., Klimont, Z., Park, I. S., Reddy, S., Fu, J. S., Chen, D., Duan, L., Lei, Y., Wang, L. T., and Yao, Z. L.: Asian emissions in 2006 for the NASA INTEX-B mission, Atmos. Chem. Phys., 9, 5131–5153, doi:10.5194/acp-9-5131-2009, 2009.

Zhang, X., Lin, Y.-H., Surratt, J. D., Zotter, P., Prévôt, A. S. H., and Weber, R. J.: Light-absorbing soluble organic aerosol in Los Angeles and Atlanta: A contrast in secondary organic aerosol, Geophys. Res. Lett., 38, L21810, doi:10.1029/2011GL049385, 2011.

ACPD
13, 19625–19648, 2013

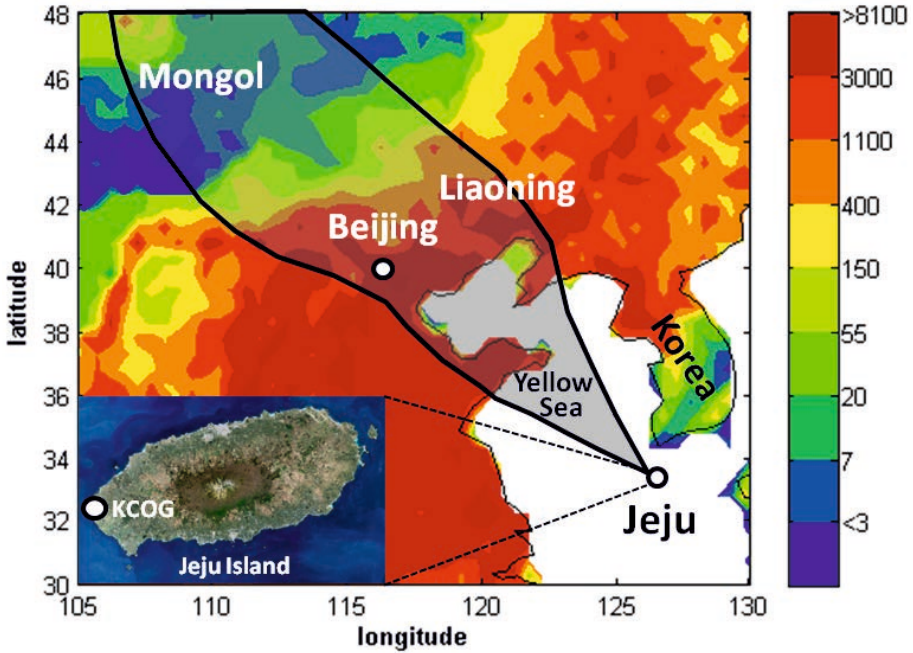

Fig. 1. Map depicting bottom-up emission inventory estimates of anthropogenic Total Organic Carbon (TOC) estimated as the sum of black carbon (BC) and organic carbon (OC) in tons yr^{-1} per $0.5^{\circ} \times 0.5^{\circ}$ grid in year 2006 (Zhang et al., 2009). The five main geographical source regions from back trajectories (BTs) analysis for the present March 2011 campaign (GoPoEx – Gosan Pollution Experiment) are indicated: Beijing, Liaoning, Mongol, Yellow Sea and Korea. The shaded sector between the black lines show the predominant range of BTs of the Chinese outflow for the study period. The location of the Korean Climate Observatory at Gosan (KCOG) on Jeju Island is shown in the inset satellite image, provided by NASA (http://earthobservatory.nasa.gov/IOTD/view.php?id=35900).

ACPD
13, 19625–19648, 2013

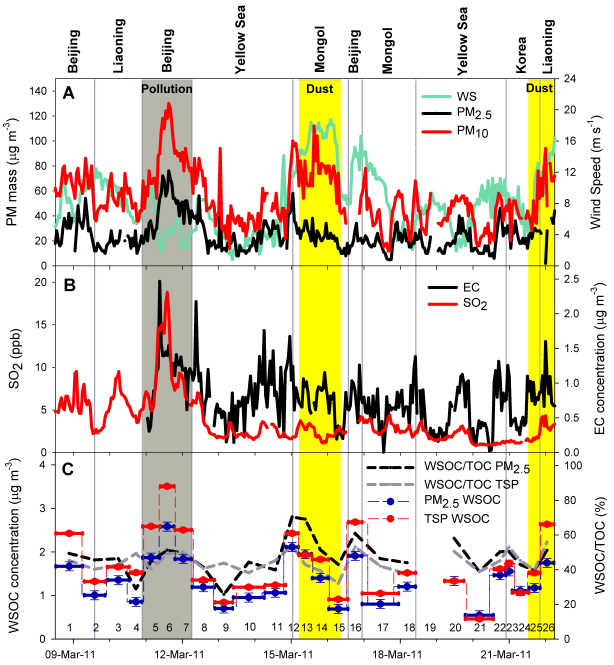

Fig. 2. Pollutant tracers and water-soluble organic (brown) carbon concentrations during the March 2011 GoPoEx campaign at KCOG: Ambient air particulate mass ($PM_{2.5}$ and PM_{10}) and wind speed **(A)**; concentrations of SO_2 provided by South Korean National Institute of Environmental Research (NIER) and semi-continuously measured elemental carbon (EC) **(B)**; concentrations of water-soluble organic carbon (WSOC) and WSOC to total organic carbon (TOC) ratio **(C)** in both ambient total suspended particles (TSP) and $PM_{2.5}$ fractions at KCOG during the GoPoEx campaign. The relation between pollutant tracers and back trajectory source regions are marked at the top. The pollution event is marked in grey and the dust events in yellow.

ACPD
13, 19625–19648, 2013

Sources and light absorption of water-soluble brown carbon aerosols

E. N. Kirillova et al.

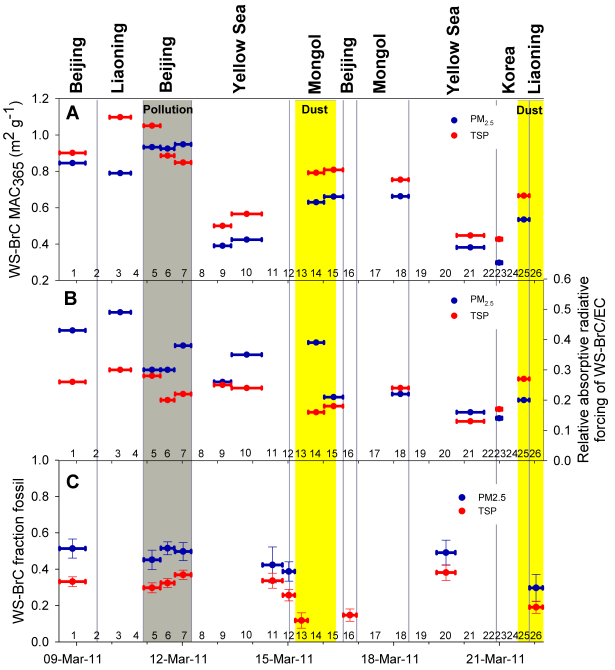

Fig. 3. Mass absorption cross section of water-soluble brown carbon (WS-BrC) at 365 nm (MAC_{365}) **(A)**; relative absorptive radiative forcing of WS-BrC compared to that of elemental carbon (EC) **(B)**; radiocarbon-based source-apportionment measurements of fraction fossil in $PM_{2.5}$ and TSP aerosols at KCOG station during the GoPoEx campaign **(C)**.

ACPD
13, 19625–19648, 2013

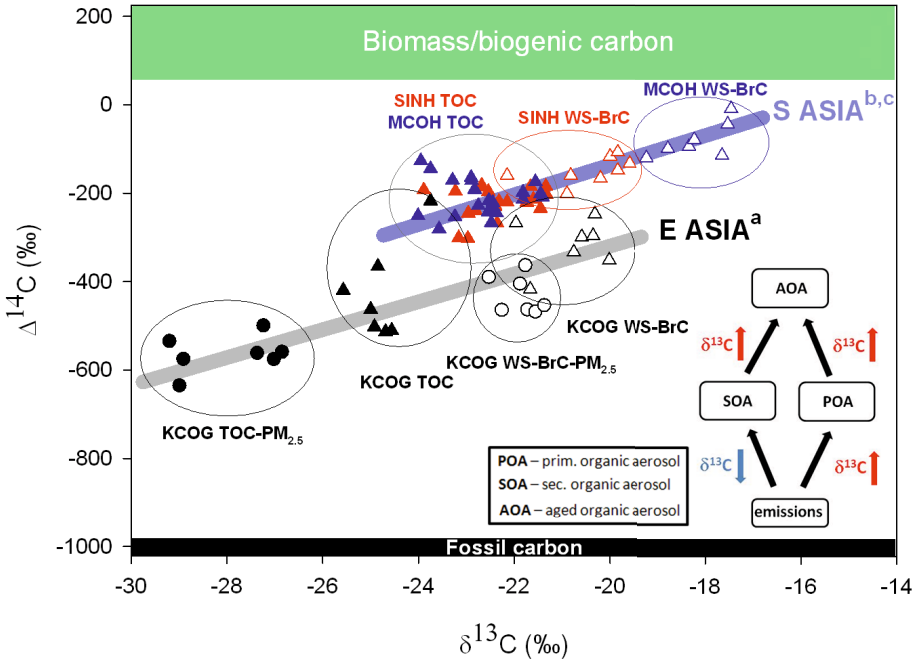

Fig. 4. Two-dimensional presentation of dual-isotope (δ^{13}C vs Δ^{14}C) signals of WS-BrC and TOC in $PM_{2.5}$ and TSP for a. GoPoEx campaign in E Asia (dust-influenced samples are excluded) compared to in S. Asia (b. Sheesley et al. (2012) and c. Kirillova et al. (2013) datasets from NW Indian site in Sinhagad (SINH) and Indian Ocean site on Hanimaadhoo Island, Maldives (MCOH). The bottom right inset graphically summarizes the general trends of the influence of atmospheric processing on the δ^{13}C signature of carbonaceous aerosols.

ACPD
13, 19625–19648, 2013

Sources and light absorption of water-soluble brown carbon aerosols

E. N. Kirillova et al.